The Tautomeric State of Histidines in Myoglobin

Shibani Bhattacharya, Steven F. Sukits, Kristen L. MacLaughlin, and Juliette T. J. Lecomte
Department of Chemistry and the Center for Biomolecular Structure and Function, The Pennsylvania State University, University Park, Pennsylvania 16802 USA

ABSTRACT ^{1}H–^{15}N HMQC spectra were collected on ^{15}N-labeled sperm whale myoglobin (Mb) to determine the tautomeric state of its histidines in the neutral form. By analyzing metaquoMb and metcyanoMb data sets collected at various pH values, cross-peaks were assigned to the imidazole rings and their patterns interpreted. Of the nine histidines not interacting with the heme in sperm whale myoglobin, it was found that seven (His-12, His-48, His-81, His-82, His-113, His-116, and His-119) are predominantly in the Nϵ2H form with varying degrees of contribution from the Nδ1H form. The eighth, His-24, is in the Nδ1H state as expected from the solid state structure. ^{13}C correlation spectra were collected to probe the state of the ninth residue (His-36). Tentative interpretation of the data through comparison with horse Mb suggested that this ring is predominantly in the Nδ1H state. In addition, signals were observed from the histidines associated with the heme (His-64, His-93, and His-97) in the ^{1}H–^{15}N HMQC spectra of the metcyano form. In several cases, the tautomeric state of the imidazole ring could not be derived from inspection of the solid state structure. It was noted that hydrogen bonding of the ring was not unambiguously reflected in the nitrogen chemical shift. With the experimentally determined tautomeric state composition in solution, it will be possible to broaden the scope of other studies focused on the electrostatic contribution of histidines to the thermodynamic properties of myoglobin.

INTRODUCTION

Myoglobin (Mb) from sperm whale muscle is a water-soluble protein containing 153 amino acid residues. An unusually high number of these, twelve, are histidines which interact with specific partners and exhibit various degree of solvent accessibility in the native state. As a consequence of their dissimilar microenvironments, the histidines of Mb have ionization constants more or less shifted from the exposed side chain value. This characteristic has long been recognized and has made Mb an appealing model system for studies of electrostatic interactions. Numerous investigations, experimental and computational, have been aimed at understanding the principal determinants of histidine pK_a values in this protein (Shire et al., 1974; Botelho et al., 1978; Friend and Gurd, 1979a,b; García-Moreno et al., 1985; Bashford et al., 1993; Yang and Honig, 1994). Of special relevance to the present work are proton NMR pH titrations of horse and sperm whale metaquoMb and apoMb, which were performed to determine individual ionization constants at room temperature in the absence of added salt (Cocco et al., 1992). These titrations have been complemented with others at various NaCl concentrations (Kao, 1994) and as a function of temperature (Bhattacharya and Lecomte, 1997).

For the same reasons that the microenvironment of a histidine dictates the ionization constant under one set of conditions, the microenvironment also controls the sensitivity of the constant to variations of temperature and salt concentration. To interpret completely the thermodynamic parameters of histidine ionization and their response to these external factors, it is necessary to compare the results for each residue to an adequate reference state. One useful reference state for purposes of free energy decomposition takes explicitly into account the influence of the native environment on the availability of the imidazole nitrogens for protonation. Such a reference state is an ideal imidazole moiety in the tautomeric mixture imposed by the native fold (Botelho et al., 1978; Shire et al., 1974; Bashford et al., 1993).

Upon losing a proton, the imidazolium cation (Scheme 1 *A*) produces two different tautomers of imidazole: that with a free Nδ1 site (Scheme 1 *B*; see Scheme 1 *D* for atom nomenclature) and that with a free Nϵ2 site (Scheme 1 *C*). Studies of histidine methylated at either the Nϵ2 or the Nδ1 atom have shown that the two sites have distinct microscopic binding constants for the proton, Nϵ2 being ~0.6 pH unit more basic than Nδ1 (Reynolds et al., 1973; Boschcov et al., 1983; Tanokura, 1983). As listed in Table 1, the difference in pK_a values has both enthalpic (N–H bond strength) and entropic (accessibility to solvent) components (Boschcov et al., 1983). The latter emphasizes the role of solvation in modulating the properties of the imidazole group. The equilibrium established between the two states in solution therefore makes contributions to the macroscopic pK_a that cannot be overlooked.

Received for publication and in final form

Address reprint requests to Dr. Juliette T. J. Lecomte, The Pennsylvania State University, Chemistry Department, 152 Davey Laboratory, University Park, PA 16802. Tel.: 814-863-1153; Fax: 814-863-8403; E-mail: jtl1@psu.edu.

Abbreviations used: apoMb, apomyoglobin; CT, constant time; DSS, sodium 2,2-dimethyl-2-silapentane-5-sulfonate; HMQC, heteronuclear multiple quantum coherence; HSQC, heteronuclear single quantum coherence; IPTG, isopropyl-β-D-thiogalactopyranoside; Mb, myoglobin; MbCO, carbonmonoxymyoglobin; metMb, ferrimyoglobin; metMbCN, metcyanomyoglobin; metaquoMb, metMbH_2O, metaquomyoglobin; NMR, nuclear magnetic resonance; NOE, nuclear Overhauser effect; NOESY, two-dimensional nuclear Overhauser spectroscopy; TOCSY, total correlation spectroscopy; TPPI, time proportional phase incrementation.

0006-3495/97/12/3230/11 $2.00

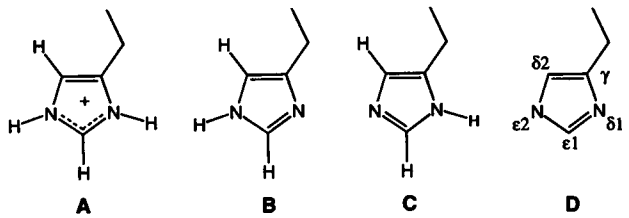

Scheme 1.

Free histidine forms a mixture with a 4:1 preference for Nδ1 deprotonation (Scheme 1 *B*) (Reynolds et al., 1973); however, the environments defined by a native protein fold often favor different proportions. In extreme cases, steric crowding, hydrogen bonding, and other local interactions may effectively restrict the protonation-deprotonation reaction to one or the other nitrogen. Assumptions about the hydrogen-bonding networks and the most accessible nitrogen sites are generally formulated on the basis of neutron diffraction or x-ray structures. The drawback of this approach is that the tautomeric composition in the solid state might not hold in the solution phase given the variability in the conformation of many protein side chains when the crystal packing forces are disrupted and the solvent is allowed to rearrange (Smith et al., 1989). In this context, the utility of NMR spectroscopy in extracting the necessary information has been well documented.

Several NMR observables of the imidazole ring are sensitive to tautomeric composition: short- and long-range ^{13}C–^{1}H coupling constants (Wasylishen and Tomlinson, 1975, 1977), ^{15}N–^{1}H, and ^{13}C–^{15}N coupling constants (Blomberg et al., 1977), ^{13}C chemical shift (Reynolds et al., 1973), and ^{15}N chemical shift (Alei et al., 1980). Wilbur and Allerhand (1977) inspected the tautomeric states in Mb from various animal species by monitoring the Cγ shift with natural abundance ^{13}C NMR spectroscopy. This pioneering study suffered from two disadvantages: assigning individual histidine signals by one-dimensional methods alone and interpreting ^{13}C chemical shifts unambiguously. With isotopic enrichment, the ^{15}N chemical shift method has proven to be especially suitable for proteins. It has been applied to diamagnetic (van Dijk et al., 1990, 1992; Annand et al., 1993; Pelton et al., 1993; Plesniak et al., 1996; Garrett et al., 1997a,b) as well as paramagnetic proteins (Xia et al., 1995) to address mechanistic issues and characterize structural details in solution. The latter application is also that of the present study, with the ultimate goal of constructing and testing thermodynamic and electrostatic models for proton binding at histidine sites.

The success and reliability of the ^{15}N chemical shift method made it an excellent choice for the description of the titrating histidines in Mb. The data presented in this study provide an estimate of the tautomeric proportions for the imidazole rings. This proportion is found to be a sensitive probe for the local interactions involving the side chain. In addition, the protonation state of the masked histidines (those that do not titrate over the native pH range) is assigned. It is shown that the deductions based on the x-ray or neutron diffraction data may not be appropriate for detailed modeling of the properties of the protein in solution. The tautomeric state information and the structural details obtained through this study will be crucial in the thermodynamic analyses of ionization constant response to salt (Kao, 1994) and temperature (Bhattacharya and Lecomte, 1997).

TABLE 1 Thermodynamic parameters for histidine and derivatives

	pK_a	$\Delta H°$ (kJ mol^{-1})	$\Delta S°$ (J mol^{-1} K^{-1})
His	6.14	28.5 ± 0.8	−23 ± 3
Nδ1-MeHis	6.61	31.0 ± 0.8	−22 ± 2
Nε2-MeHis	5.99	24.3 ± 0.4	−33 ± 1

Values are at 298 K in H_2O taken from Boschcov et al. (1983).

MATERIALS AND METHODS

Protein preparation and purification

All chemicals were purchased from Sigma Chemical Co. (St. Louis, MO) except those isotopically labeled, which were from Isotec (Miamisburg, OH). The gene for sperm whale (*Physeter catodon*) myoglobin contained in a pET13d plasmid was a generous gift of Dr. Fong Shu, Brookhaven National Laboratory. The gene was sequenced and confirmed to correspond to the desired protein. Overexpression was achieved in *Escherichia coli* cell strain BL21 (DE3), which was transformed following the $CaCl_2$ method (Sambrook et al., 1989). A 60-ml starter growth of M9 minimal medium was inoculated from a freshly transformed M9 plate and incubated with shaking for 22 h at 37°C, and 10 ml of starter growth was then added to each of the four flasks containing 500 ml of M9 supplemented with $^{15}NH_4Cl$ as the sole source of nitrogen (or $^{15}NH_4Cl$ and ^{13}C-glucose for doubly labeled protein). The cells were incubated at 37°C with shaking until the OD_{600} reached 0.7–0.9 (3.5–5 hr). Protein production was induced by the addition of IPTG to a final concentration of 0.5 mM. After induction, the cells were incubated with shaking for 7 h at 25°C to produce soluble apomyoglobin. The cells were harvested after centrifugation at 11,325 × *g* for 20 min. Protein extraction and reconstitution with heme was performed according to the reported protocol (Tolman et al., 1995). Myoglobin was purified in a two-step process involving a cation exchange column (DEAE, 20 mM Tris buffer, pH 8) and sizing column (G75, 20 mM Tris buffer, pH 8). Unlabeled protein was prepared according to the same protocol with unlabeled nutrients.

NMR samples

A 9-mg amount of uniformly ^{15}N-labeled protein was dissolved in 500 μl of 90% H_2O/10% $^{2}H_2O$, yielding a ~1 mM protein sample. For ^{13}C heteronuclear experiments, the ^{13}C,^{15}N-labeled protein was dissolved in 99.9% $^{2}H_2O$. All solutions were allowed to reach equilibrium for heme orientation within the protein (La Mar et al., 1984). The pH was adjusted using 0.1 M NaOH (or $NaO^{2}H$) and 0.1 M HCl (or ^{2}HCl). The solutions were not buffered for consistency with previous work. The pH was measured before and after the experiments, and the average of the two values is reported. The metcyano form of Mb was obtained by adding a crystal of KCN to metaquoMb. The apoprotein of the ^{15}N-labeled protein was prepared by the 2-butanone method (Teale, 1959) as described elsewhere (Lecomte and Cocco, 1990).

NMR experiments

All data were recorded on a Bruker AMX2–500 spectrometer operating at a ^{1}H frequency of 500.13 MHz, ^{13}C frequency of 125.76 MHz, and ^{15}N frequency of 50.68 MHz. ^{1}H–^{15}N HMQC spectra (Müller, 1979; Bodenhausen and Ruben, 1980) of metaquoMb and metcyanoMb were acquired with a 22-ms delay for selective observation of the long-range proton-nitrogen correlation of histidines ($^2J_{N-H}$ = 6–12 Hz). A total of 2048 complex points with a spectral width of 7042 Hz was acquired in the proton dimension. The proton spectral width was increased to 25,000 Hz to observe the paramagnetically downfield shifted signals in metcyanoMb. The ^{1}H carrier was placed on the water resonance, and presaturation was applied for 1.2 s. A total of 256 complex points (States-TPPI quadrature detection) was acquired in the indirectly detected ^{15}N dimension. The ^{15}N spectral width was 150 ppm (7602 Hz), centered at 225 ppm. A minimum of 128 transients was acquired per point; this number was increased as the sample was diluted by pH adjustments.

A ^{1}H–^{15}N HSQC spectrum (Bodenhausen and Ruben, 1980) of metaquoMb at high pH was acquired with gradient-enhanced water suppression using a modified WATERGATE sequence (Piotto et al., 1992) and a binomial excitation delay of 90 μs. The INEPT delay was set to 2.3 ms for observation of single-bond couplings ($^1J_{N-H} \approx 90$ Hz). Parameters were as above for the ^{1}H dimension; for the indirect dimension, the carrier was placed at 135 ppm. A total of 128 real points (TPPI quadrature detection) was collected with a minimum of 32 transients per point.

^{1}H–^{13}C CT-HSQC data sets (Vuister and Bax, 1992) were collected on ^{15}N,^{13}C-labeled metaquoMb at pH 5.4 and 313 K. The constant time delay was 16.7 ms (corresponding to $^1J_{C-C}$ of 70 Hz) so as to distinguish Cδ2H and Cϵ1H cross-peaks according to their phase (Plesniak et al., 1996). Loss of signals at high pH required acquisition of ^{1}H–^{13}C HMQC data as well. The latter were collected with a 3.6-ms delay ($^1J_{C-H}$ = 220–180 Hz). The parameters were otherwise identical; ^{13}C carrier placed at 101 ppm with a spectral width of 100 ppm (12,500 Hz). A total of 256 pairs of data points was acquired with 128 (CT-HSQC) or 256 (HMQC) transients per point with TPPI-States quadrature detection in the indirect dimension.

Homonuclear data (^{1}H-^{1}H NOESY and ^{1}H-^{1}H TOCSY) were acquired as described elsewhere (Lecomte et al., 1996; Bhattacharya and Lecomte, 1997) to confirm some of the assignments in the metaquo and metcyano form at the matching temperature. The proton spectral widths were adjusted to include the paramagnetically shifted signals when necessary.

All data were processed with FELIX or NMRPipe (Molecular Simulations, San Diego, CA). Data collected in 90% H_2O/10% ^2H_2O were subjected to a sinebell-based convolution function to suppress the solvent. Data were multiplied by shifted (45° to 60°) squared sinebell functions in both dimensions and were zero-filled so as to achieve a digital resolution of ~7 Hz/point in the ^{1}H dimension (narrow spectral width), 7 Hz/point in the ^{15}N dimension, and 12.5 Hz/point in the ^{13}C dimension. The proton chemical shifts were indirectly referenced to DSS through the water signal with temperature correction (Wishart et al., 1995). The probe temperature was calibrated by using neat ethylene glycol as a standard (Martin et al., 1980). Nitrogen shifts were referenced indirectly to ammonium chloride (Live et al., 1984), and carbon to DSS. In the text, the nuclei of interest are underlined wherever ambiguity could arise.

RESULTS AND DISCUSSION

Several solid-state structure determinations of myoglobin in various complexation states have been carried out at moderately acidic pH values (Takano, 1977a,b; Phillips, 1980; Cheng and Schoenborn, 1991). Of interest to this study is the high-spin (S = 5/2) ferric metaquoMb complex (Takano, 1977a; Takano, 1984), which yields well resolved proton NMR spectra at pH 5.7. This pH was used to obtain the necessary spectral assignments and to compare the solution structure with the x-ray structure (Kao and Lecomte, 1993). In metaquoMb, protons located within 12 Å of the iron atom experience efficient paramagnetic relaxation and their signals and NOEs are not readily detected. Three histidines fall within this radius in the sperm whale protein: His-64 (E7 or distal), His-93 (F8 or proximal), and His-97 (FG3). The other histidines are His-12 (A10), His-24 (B5), His-36 (C1), His-48 (CD6), His-81 (EF4), His-82 (EF5), His-113 (G14), His-116 (G17), and His-119 (GH1). These have been assigned and are detectable by homonuclear two-dimensional methods under most pH conditions (Cocco et al., 1992). Fig. 1 presents the curves obtained in a typical proton titration experiment of sperm whale metaquoMb. Proton titration curves such as these have provided the ionization constants listed in Table 2 (Cocco et al., 1992).

To further the characterization of histidines, ^{15}N data were collected at the pH values indicated by arrows on Fig. 1. Histidine ^{15}N chemical shifts can be determined by two-dimensional correlation experiments utilizing $^2J_{N-H}$ and $^3J_{N-H}$ couplings (Sudmeier et al., 1996). The ^{1}H–^{15}N HMQC spectrum is adequate to identify the various forms of histidines (Pelton et al., 1993). In this experiment, the pure tautomers give distinct ^{1}H-^{15}N coupling patterns (discussed in the cases of His-24 and His-119 below), and mixtures can be characterized semiquantitatively with ^{15}N

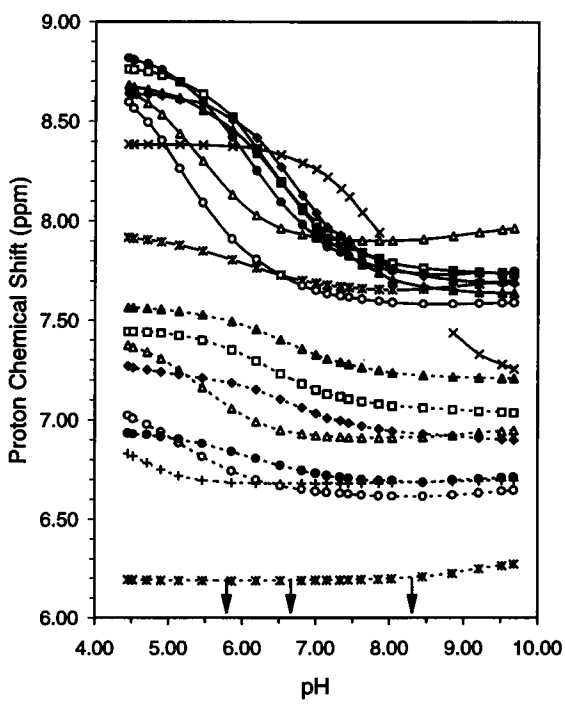

FIGURE 1 Typical proton titration curves for the histidines of sperm whale metaquoMb at 298 K and in the absence of added salt. The assignments were confirmed by two-dimensional data as described previously (Cocco et al., 1992) and are as follows: His-24, ✳; His-82, +; His-113, ○; His-119, ●; His-48, △; His-81, ◆; His-12, □; His-116, ▲; His-36, ×. The data points are connected by lines to guide the eye: · · ·, Cδ2H signals; ——, Cϵ1H signals. The three arrows on the pH axis indicate the values at which ^{1}H–^{15}N HMQC spectra were collected: 5.7, 6.6, and 8.3. The pK_a values obtained from this type of curves are reported in Table 2 (Cocco et al., 1992).

TABLE 2 Ionization constants and structural parameters for histidines in Mb

Residue	pK_a*	Distance to iron atom# Nδ1	Distance to iron atom# Nε2	Solvent accessibility§ (%) Nδ1	Solvent accessibility§ (%) Nε2
His-12	6.4	27	27	75	40
His-24	<4.8	18	19	0	0
His-36	8.2	16	16	25	40
His-48	5.5	16	17	20	60
His-64	<5¶	6.1	4.5	5	0
His-81	6.7	23	25	30	100
His-82	<4.8	16	16	5	0
His-93	<5¶	4.3	2.2	0	0
His-97	5.6¶	6.6	5.7	30	0
His-113	5.4	20	20	50	45
His-116	6.6	25	26	0	100
His-119	6.1	23	21	25	0

*Values for sperm whale metaquoMb, at 298 K with no salt added (Cocco et al., 1992), except where noted.
#Distance in Å calculated from the refined structure of sperm whale metaquoMb (Brookhaven Protein Data Bank file 4MBN; Takano, 1984), with protons added with the program X-PLOR (Brünger, 1992).
§Static solvent accessibility normalized to exposed tripeptide (Lee and Richards, 1971).
¶Value for sperm whale MbCO at 308 K from Bashford et al. (1993).

chemical shift values (van Dijk et al., 1992). Three types of histidine nitrogens can be classified by their representative chemical shifts (Witanowski et al., 1972; Blomberg et al., 1977; Bachovchin, 1986; Pelton et al., 1993): deprotonated N (=N−, type β), 249.5 ppm; protonated in a neutral ring (NH, type α), 167.5 ppm; and protonated and charged N in a positively charged ring (NH^+, type $\alpha+$), 176.5 ppm.

The ^1H–^{15}N HMQC spectra of metaquoMb allowed for the determination of the predominant tautomeric state of only five of the nine observable histidines in the neutral state. When the pH is raised above 8, the metaquo form starts to convert noticeably into the methydroxy form of the protein (pK ≈ 8.8; Brunori et al., 1968; McGrath and La Mar, 1978), leading to a significant decrease of the metaquoMb population and broad lines. To complement the metaquo data in the high pH range, spectra were collected on the metcyano form of Mb, a low-spin (S = 1/2) ferric complex stable at high pH. Spectral assignments for the three histidines near the heme in this complex were obtained from the work of La Mar and co-workers (Cutnell et al., 1981; Emerson and La Mar, 1990). The histidines remote from the heme were identified either by proton NOEs typical of each histidine (Cocco et al., 1992; Kao, 1994) or by chemical shift comparisons.

His-24

According to the x-ray and neutron diffraction structures of myoglobin, His-24 is completely buried in the protein and its Nδ1H forms a hydrogen bond with the carbonyl group of Asp-20. His-24 is thought to form a second hydrogen bond in which its Nε2 serves as an acceptor for the Nε2*H* of His-119 (Takano, 1977a, 1984; Cheng and Schoenborn, 1991). Thus, the solid-state data leave little doubt about the status of His-24 in solution, and both nitrogens are likely to be involved in strong hydrogen bonds. In fact, there is ample NMR evidence to suggest that, in sperm whale Mb, the 20–24-119 triad of hydrogen-bonded residues maintains its relative spatial relationship in solution through the entire accessible pH range (Dalvit and Wright, 1987; Cocco et al., 1992; Kao, 1994; Lecomte et al., 1996; Yamamoto, 1996).

His-24 is a masked histidine (Breslow, 1964). Its protonation requires the placement of a positive charge within a hydrophobic site and the disruption of its interaction with His-119. These events are expected to take place at low pH and to be accompanied by B-GH interface structural alterations (Barrick et al., 1994). In agreement with the low pK_a, the proton chemical shifts of His-24 are practically invariant with pH (Fig. 1). The deviation exhibited by Cε1H as the pH is lowered below 7 is interpreted as a secondary effect due to the titration of His-119.

Fig. 2 *A* contains the ^1H–^{15}N HMQC spectrum of metaquoMb at pH 8.3. The pattern observed for His-24 has four connectivities: Cδ2H–Nε2, Cδ2H–Nδ1H (the latter being weak), and Cε1H–Nε2, Cε1H–Nδ1H (comparable intensities). The direct connectivity between Nδ1 and its attached proton is observed in the ^1H–^{15}N HSQC spectrum (not shown, see Fig. 4 *B*). The detection of the slowly exchanging Nδ1H signal supports the presence of the side-chain: main-chain hydrogen bond to Asp-20 (Yamamoto, 1996). The five cross-peaks and the nitrogen separation in Fig. 2 *A* are consistent with the formation of the Nδ1H tautomer (Scheme 1 *C*).

Lowering the pH to 5.7 (Fig. 2 *B*) does not change the pattern of His-24, although the Cε1H–Nε2 cross-peak begins to broaden in the proton and nitrogen dimensions. The Nδ1H is well protected from exchange, and its signal remains visible down to this pH. This is noteworthy in view of the fast exchange generally exhibited by these labile hydrogens (Wüthrich, 1986). The Nε2 (type β) chemical shift of His-24 undergoes an upfield shift as the pH is lowered from 8.3 to 5.7. A likely interpretation is that the state of protonation of His-119 influences this chemical shift through the Nε2-H–Nε2 hydrogen bond.

The difference between the observed ^{15}N chemical shift and the standard value for the corresponding nitrogen type has been used to identify H-bond formation in model compounds (Shuster and Roberts, 1979; Roberts et al., 1982; Farr-Jones et al., 1993) and proteins (Bachovchin, 1986; Bachovchin et al., 1988). According to the model compound studies, a type-β nitrogen moves upfield (in the direction of protonation) when behaving as an acceptor, whereas a type α or $\alpha+$ nitrogen moves downfield (in the direction of deprotonation) when behaving as a donor. The magnitude of these shifts can reach 10 ppm. If His-24 conformed to the rule, the separation between the type α and type β nitrogens should be measurably reduced with respect to the unperturbed 82 ppm α-β difference. This is barely the

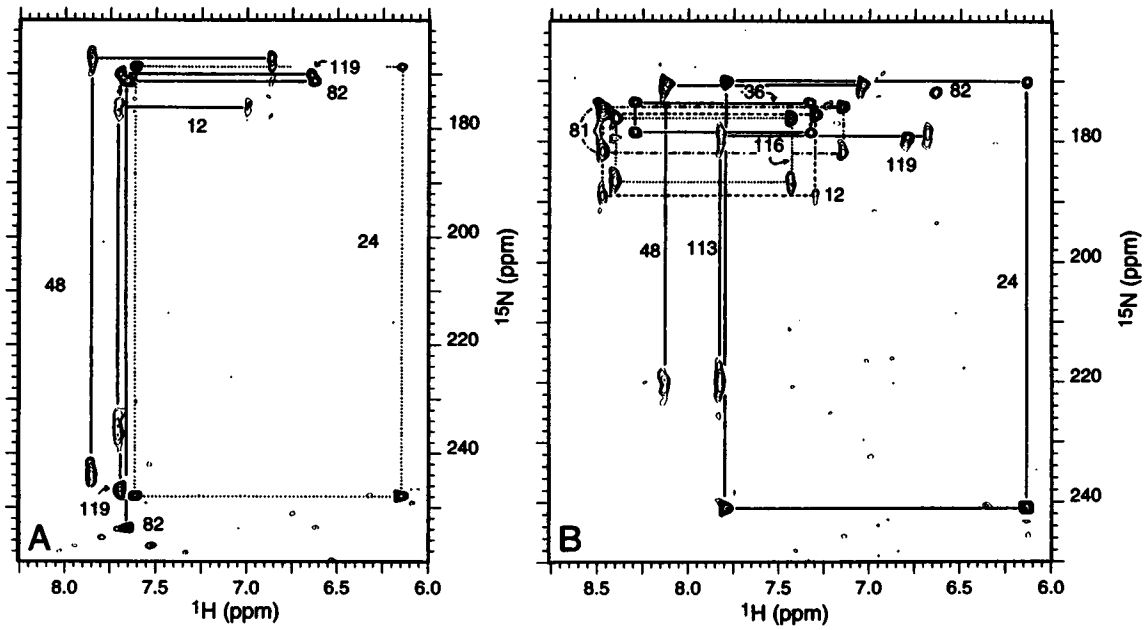

FIGURE 2 (*A*) ^{1}H–^{15}N HMQC spectrum of ^{15}N-labeled metaquoMb at pH 8.3 and 298 K in 90% H_2O/10% $^{2}H_2O$. Cross-peaks belonging to the same residue are connected with lines. The only residue for which all four connectivities are observed is His-24 (· · ·). (*B*) Same as *A*, with pH adjusted to 5.7. The only residue yielding a pattern characteristic of a fully protonated imidazole group is His-36. In this spectrum, a larger number of residues is detectable compared with the higher pH spectrum.

case (Table 3). It is possible that for some histidines in proteins, the shifts cannot be compared meaningfully to those of model compounds. This could be due to compensatory shifts induced by the nonpolar characteristics of the local environment, counteracting the chemical shift changes associated with H-bond formation (Farr-Jones et al., 1993). Similar discrepancies between the expectations raised by the model compounds and the actual protein chemical shifts have been reported by others (Pelton et al., 1993). In summary, the NMR observations support that His-24 is hydrogen bonded in the neutral state through its δ1 and ϵ2 nitrogens and that the Nδ1H tautomer exists throughout the native pH range. The fact that hydrogen bonding is not unambiguously reflected in the nitrogen shifts illustrates

TABLE 3 Chemical shifts and tautomeric forms for histidines in Mb

		^{15}N chemical shift (ppm)		^{1}H chemical shift (ppm)		
Residue	Conditions	Nδ1	Nε2	Hδ2	Hε1	State
His-12	metMbH_2O*	236#	176#	7.00	7.71	
	metMbCN§	235.4	177.7	6.91	7.66	Nε2H, 90%
His-24	metMbH_2O	168.7	248.0	6.15	7.61	
	metMbCN	169.4	248.6	6.37	7.74	Nδ1H, 100%
His-36	metMbH_2O	178.6	173.7	7.33	8.30	Nδ1H (80%)¶
His-48	metMbH_2O	244.2	167.0	6.87	7.86	
	metMbCN	242.9	169.2	7.09	8.21	Nε2H
His-64	metMbCN		182.8	11.55		(Nε2H)‖
His-81	metMbCN	228.5	182.9	6.85	7.66	Nε2H, 80%
His-82	metMbH_2O	253.8	171.5	6.63	7.66	
	metMbCN	254.1	171.9	6.84	7.61	Nε2H
His-93	metMbCN	184.7				(Nε2H)‖
His-97	metMbCN	246.2	169.1		6.79	(Nε2H)‖
His-113	metMbCN	222#	186.8	6.75	7.62	Nε2H, 70%
His-116	metMbCN	224#	190.1	7.15	7.61	Nε2H, 60%
His-119	metMbH_2O	246.7	170.7	6.65	7.70	Nε2H, 100%

*Data for metMbH_2O at pH 8.3 and 298 K, except for His-36 (pH 5.7 and 298 K).
#Approximate values (±2 ppm) because of overlap or broad line width.
§Data for metMbCN in H_2O at pH 10.3 and 304 K, except for His-93 (pH 8.3 and 298 K).
¶Obtained through ^{13}C data; see text.
‖Based on the crystal structure; see text.

that caution should be exercised in the interpretation of buried histidine data.

His-119

His-119, the partner of His-24, is expected to adopt the Nϵ2H tautomer when in the neutral state (Scheme 1 *B*). The Nδ1 site is partially exposed to solvent and available for protonation (Table 2). The predominance of the Nϵ2H tautomer at basic pH is indeed observed in the ^{1}H–^{15}N HMQC spectrum (Fig. 2 *A*) where three cross-peaks are detected for His119: Cδ2H–Nϵ2H, Cϵ1H–Nϵ2H, and Cϵ1H–Nδ1. At the lower pH (Fig. 2 *B*), the signals for His-119 have moved, and the connectivities to Cϵ1H are lost. This result is in accordance with the pK_a of this residue (Table 2) and the broadening of the proton signals through the titration. The Nϵ2H signal of His-119 was not detected under the conditions explored for this study and those of others even at low temperature (Yamamoto, 1996). Thus, rapid exchange with solvent occurs even though the Nϵ2H environment is of reduced solvent accessibility and hydrogen bond formation with His-24 is expected. This hydrogen bond has a nitrogen for acceptor and is likely to be weaker than a hydrogen bond to a carbonyl group. As discussed for His-24, ^{15}N chemical shifts and chemical shift separation do not allow one to conclude on the state of H-bonding of this residue.

The 24–119 pair illustrates that the two types of tautomers can readily be distinguished in Mb. In addition, the pair signature is recognized not only in the metaquo form (Fig. 2, *A* and *B*) but also in the metcyano form (Fig. 3) and in the apoprotein form (not shown), where it is known to play a special role in the stability of the native fold (Barrick et al., 1994). The presence of the 24–119 interaction and the resulting tautomeric composition is consistently expected on the basis of structural data in solid state and in solution. However, the state of several other histidines is not as securely deduced. In the following discussion, each observable histidine is considered: first, those that adopt a preponderant tautomeric state; second, those that are found in mixtures; and last, those for which incomplete information was obtained.

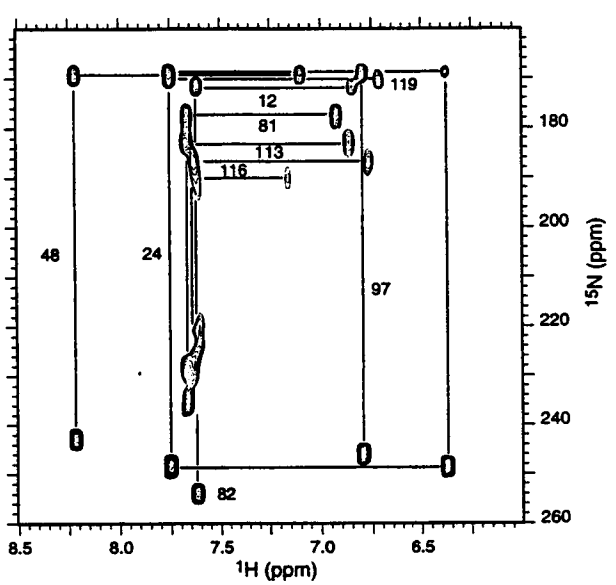

FIGURE 3 ^{1}H–^{15}N HMQC spectrum of ^{15}N-labeled metMbCN at pH 10.3 and 304 K in 90% H_2O/10% $^{2}H_2O$. Cross-peaks belonging to the same residue are connected with lines. A larger number of histidines are detectable in this form compared with the metaquo form (Fig. 2 *A*).

His-12

His-12 is in close proximity to the side chain carboxyl group of Asp-122. Asp-122 in turn interacts strongly with Lys-16. The three side chains His-12, Lys-16, and Asp-122 form a set of chargeable sites stabilizing the A helix against the GH corner (Cheng and Schoenborn, 1991). In solution, His-12 has a pK_a value close to that of an exposed histidine (Table 2). The unshifted pK_a reflects the compensating influences of nearby side chains. The ^{1}H–^{15}N–HMQC spectra shown in Figs. 2 *A* and 3 contain three equally strong cross-peaks for this histidine. No cross-peak appears between Cδ2H and the unprotonated nitrogen at 236 ppm; therefore, the Nϵ2H tautomer predominates and the Nδ1 site is available for protonation.

In the absence of strong hydrogen bonds and for a largely solvent-exposed side chain, a rough estimate of the proportion of the tautomeric states can be obtained by inspecting the chemical shift difference between the two nitrogens. When an Nϵ2H tautomer converts into an Nδ1H tautomer, both nitrogens switch between type α and type β (82 ppm apart). In mixtures, if the exchange is sufficiently fast on the chemical shift time scale, the Nδ1 and Nϵ2 nitrogens each yield a single cross-peak at the Cϵ1H frequency (and Cδ2H frequency) and the weighed average of the type α and type β nitrogen chemical shifts. If the Nϵ2H form predominates, the Nϵ2-Cϵ1H cross-peak will be biased toward the type α shift. Likewise, the Nδ1-Cϵ1H cross-peak will be biased toward the type β shift (van Dijk et al., 1992). A 1:1 mixture in fast exchange has an Nϵ2-Nδ1 difference of 0 ppm (overlapping peaks) and a 4:1 ratio in favor of the Nϵ2H tautomer (free histidine) produces ~50 ppm difference.

In the case of His-12, the three-peak pattern and the 60 ppm difference between Nϵ2 and Nδ1 signals point to a slight preference for the Nϵ2H form compared with a completely exposed, noninteracting residue. A possible partner for stabilizing the Nϵ2H form is Asp-122. In contrast, the neutron diffraction structure of MbCO at pH 5.7 has a fully deprotonated Nϵ2 (Cheng and Schoenborn, 1991) and dictates a low pK_a. The possibility of the ligation state of the iron atom influencing the pK_a is weakened by the close agreement of the values obtained in solution for MbCO (Bashford et al., 1993) and metaquoMb (Cocco et al., 1992), but it should be pointed out that the solid-state structures of Mb in different complexation states (deoxy structure 5MBN, Takano, 1984; metaquo structure 4MBN, Takano,

1984; oxy structure 1MBO, Phillips, 1980; carbonmonoxy structure 2MB5, Cheng and Schoenborn, 1991) exhibit some variability in the relative position of the GH corner (bearing Asp-122) and the A helix. The discrepancy could arise from structural alterations affecting the ionization constant and tautomeric state and raises concerns about the validity of extending solid-state observations to the solution phase.

His-48

The pK_a of His-48 is low (Table 2; Cocco et al., 1992) and an explanation for this cannot be found in most solid-state structures, which show His-48 interacting with another myoglobin molecule (Cheng and Schoenborn, 1991). A recent study by Yang and Phillips (1996) compared the x-ray structure of sperm whale myoglobin at different pH values and revealed a role for the side chain of His-48 in pH-dependent structural changes of the CD corner. In sperm whale deoxyMb, rearrangement goes as far as the formation of a hydrogen bond between Nδ1H and the main chain carbonyl of Arg-45. In solution, the intermolecular interactions are disrupted and there is some uncertainty about the exact location of the ring. NOE data in all forms of myoglobin show strong dipolar contact between Phe-46 CαH and His-48 Cε1H (Cocco et al., 1992). This indicates a preference for orientations of the ring with Nδ1 positioned toward the backbone of the CD corner. In addition, NOEs between Cε1H and the isopropyl group of Leu-49[1] confirm that one face of the ring is blocked by hydrophobic interactions. The side chain chemical shifts of Leu-49 depend on pH and provide additional evidence for facile conformational rearrangement around His-48.

The ^{15}N data indicate a preference to form the Nε2H tautomer of the neutral imidazole over that exhibited by a free histidine. According to the chemical shift values, the proportion is higher than 90%. The intramolecular interactions causing this preference are not readily identified. It is possible that a structural rearrangement reduces the accessibility of the Nδ1 site. Previous studies have relied on the Nε2 site as the principal acceptor for the proton because of relative accessibility (Table 2; Botelho et al., 1978; Friend and Gurd, 1979b), whereas our results suggest the Nδ1 site. This example emphasizes the drawbacks of interpreting microscopic properties in solution based on the structural details obtained in the solid state.

His-82

His-82 is buried and involved in an interaction with Asp-141 (H18), which stabilizes the EF corner on the H helix (Takano, 1977a). In all investigated ligation states of Mb, the environment of this residue in the solid state is practically constant. The state of protonation of His-82 is subject to two conflicting ideas. His-82 has been consistently assumed to be masked in the neutral state (Breslow, 1964; Wilbur and Allerhand, 1977) because of the energetic cost of burying it in the charged state. However, the recent neutron diffraction study of MbCO (Cheng and Schoenborn, 1991) finds His-82 fully charged at pH 5.7 and supports a high pK_a. ^1H NMR data (Fig. 1) show a slight downfield excursion at low pH. The acidic pH deflection, which becomes more pronounced when the temperature is lowered (Bhattacharya and Lecomte, 1997) and salt is added (Kao, 1994), favors but does not prove a low pK_a ionization (Cocco et al., 1992).

At basic pH, His-82 Nε2H is detected in one-dimensional ^1H spectra of metaquoMb and its assignment confirmed by observation of NOEs to Cε1H and Cδ2H (Yamamoto, 1996; this work). The one-bond connectivity between the Nε2 nitrogen and the attached proton is observed in the ^1H–^{15}N HSQC spectrum (Fig. 4 *B*). All other signals attributable to His-82 are readily found in the ^1H–^{15}N HMQC data at high pH (Fig. 2 *A*). The pattern of three cross-peaks is typical of a neutral imidazole predominantly in the Nε2H form and settles the state of His-82 at pH > 5. His-82 displays the most downfield-shifted type-β nitrogen. Its type-α nitrogen occurs at about the same value as that of His-24, His-48 and His-119. At this point there seems to be no unifying interpretation of the small variation in type α and type β shifts

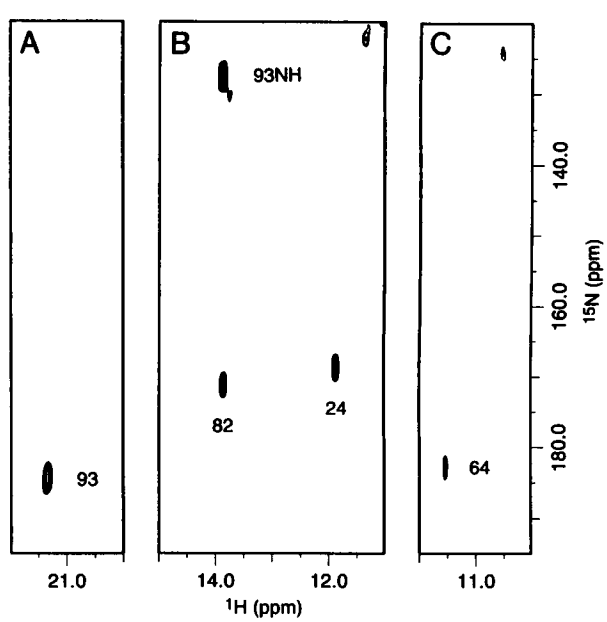

FIGURE 4 ^1H–^{15}N HMQC spectra in 90% H_2O/10% ^2H_2O of ^{15}N-^{13}C-labeled metcyanoMb at pH 8.3 and 298 K (*A* and *B*) and of ^{15}N-labeled metcyanoMb at pH 10.3 and 304 K (*C*). One-bond N-H coupling cross-peaks are labeled for His-93 (Nδ1H), His-24 (Nδ1H), His-82 (Nε2H), and His-93 (peptide NH). In *C*, the cross-peak arises from coupling between His-64 Cδ2H and Nε2H. The proton chemical shift ranges are as follows: (*A*), 20 to 22 ppm; (*B*), 11 to 15 ppm; (*C*), 10 to 12 ppm.

[1] The strength of the NOEs from His-48 Cδ2H and Cε1H to CγH of Leu-49 indicates that this proton is pointing toward the ring as seen in horse Mb (Evans and Brayer, 1990) and in the refined sperm whale deoxyMb x-ray coordinates (Brookhaven Protein Data Bank 5MBN; Takano, 1984). This is in contrast to the metaquo geometry (Brookhaven Protein Data Bank 4MBN; Takano, 1984).

based on the differences in the environment of the residues or state of hydrogen bonding.

His-24 and His-82 are similar in that they are buried and hydrogen bonded. However, their pH dependence is different. All signals of His-24 remain visible down to low pH values (Fig. 2 *B*), whereas His-82 experiences substantial broadening at pH 5.6, which renders the Cε1H connectivities undetectable. This is consistent with the broadening observed for the proton signals in one-dimensional titrations and indicates that the pK_a of His-82 is higher than that of His-24.

His-81, -113, and -116

In Fig. 3, three histidines give rise to three-peak patterns with smaller nitrogen chemical shift separation than the residues discussed above. These are from His-81, His-113, and His-116, which are therefore all found in mixtures of tautomeric states, with a predominance of the Nε2H form. His-81, the residue most resembling an exposed residue according to its pK_a and enthalpy of ionization (Bhattacharya and Lecomte, 1997), has a chemical shift difference of 46 ppm, practically corresponding to the 4:1 mixture of free histidine. The proportion of Nε2H form is reduced from this value in His-113 and reduced further in His-116. Especially for the latter, fast exchange broadening is observed in the nitrogen dimension. The x-ray structure does not offer obvious hydrogen-bonding partners that could account for the reduction of nitrogen shift separation in these three instances. In all three cases, the relative accessibility (Table 2) fails as an indicator of the mixture of states.

His-36

His-36 is the only histidine in myoglobin that has an elevated pK_a compared with a free histidine (Table 2). Intermolecular interactions in the solid state weaken the prediction of the solution properties of His-36 on the basis of x-ray structure (Botelho and Gurd, 1978). The high pK_a is presumably due to interaction with the nearby Glu-38, which would stabilize the protonated ring through Nδ1H-Oε1,2 interactions (Cheng and Schoenborn, 1991). Phe-106 adds to the complexity of the site by docking against His-36, limiting its accessibility to solvent, and possibly providing π electron density favoring the imidazolium cation (Loewenthal et al., 1992). At pH 5.6, His-36 is the only fully protonated histidine. The ^1H–^{15}N HMQC spectrum at this pH (Fig. 2 *B*) contains four cross-peaks (Cδ2H–Nε2H, Cδ2H–Nδ1H, Cε1H–Nε2H, and Cε1H–Nδ1-H) in a pattern expected of a protonated imidazole (Scheme 1 *A*). On the basis of the interaction with Glu-38, Nδ1 is assigned the type $\alpha+$, at 178.7 ppm.

His-36 proton signals experience substantial broadening throughout the titration, to an extent that prevents detection in the transition zone at room temperature (Cocco et al., 1992; Bhattacharya and Lecomte, 1997). In the metaquoMb ^1H–^{15}N HMQC spectra, His-36 is not observed at pH 8.3 probably for the same reason. Even at pH 10.3 in the metcyano form, ~2 pH unit above the pK_a of the residue, the signals of His-36 are not seen. As the signals are observable in the protonated form, paramagnetic effects are not responsible for the disappearance. It is likely that the tautomeric equilibrium is such that the nitrogen signals are broadened beyond detection.

In an effort to obtain information on the predominant tautomeric form of His-36 in the neutral state, an alternate strategy had to be adopted. Even though Nδ1 and Nε2 signals are not detected, Cε1 and Cδ2 signals might be. ^1H–^{13}C HMQC as well as ^1H–^{13}C CT-HSQC data were collected at high pH. The ^1H–^{13}C CT-HSQC spectrum contained only a few Cδ2H cross-peaks, whereas most of these appeared in the ^1H–^{13}C HMQC spectrum. By using previous assignments, titration curves, and several TOCSY data sets collected above and below pH 8.7 and at 313 K, the Cε1H cross peak of His-36 was identified in all ^1H–^{13}C correlation experiments. However, the broad Cδ2H cross-peak remained elusive. Tentative analysis indicates that both His-36 carbons shift downfield as the pH is raised, implying a larger than normal proportion of the Nδ1H tautomer (Reynolds et al., 1973). This view is supported by data on equine metaquoMb, where the entire titration was monitored by ^{13}C and ^1H shifts at 313 K (Bhattacharya and Lecomte, 1997). A reasonable explanation of the perturbation of the tautomeric equilibrium in both proteins may be based on the interactions between His-36 Nδ1H and the carboxylic oxygens of Glu-38.

His -97, -64, and -93

The metcyano form offers the opportunity to inspect signals from histidines close to the heme. For example, the Cε1H of His-97 (7.2 Å from the iron atom) resonates at 6.8 ppm (Fig. 3) (Emerson and La Mar, 1990), and its relaxation time is long enough that ^2J correlations are detected to both ring nitrogens. The separation of the cross-peaks in the nitrogen dimension indicates the formation of a pure tautomeric form. The Cδ2H (4.7 Å from the iron atom) relaxes too rapidly for the remaining correlations to be detected. It can be assumed that the Nε2H tautomer exists because His-97 interacts through the Nε2 site with the oxygen atom(s) of the heme propionate-A group (Takano, 1977a).

Also visible in the metcyano form at high pH is the Cδ2H of His-64 (6.3 Å from the iron atom) at 11.55 ppm. In this case, a single cross-peak is observed at the frequency of an α-nitrogen (Fig. 4 *C*), suggesting that the residue is unprotonated in agreement with the low pK_a of the distal histidine (Morikis et al., 1989). Accordingly, the missing cross-peak between Cδ2H and a β-nitrogen points to the formation of the Nε2H tautomer. This form could be stabilized in preference to the other by a hydrogen bond to the cyanide ligand (Lecomte and La Mar, 1987) as well as other steric constraints.

The Nδ1H of the proximal histidine is 5.2 Å from the iron. It participates in a hydrogen bond to the backbone carbonyl of Ser-92. The exchange of this proton is base-catalyzed only and the signal is clearly observed at 21.4 ppm in metMbCN at low pH (Cutnell et al., 1981). A $^1J_{N-H}$ correlation cross-peak is observed at 185 ppm in the ^1H–^{15}N HMQC spectra (Fig. 4 *A*). The tautomeric state of this histidine is not open to question as coordination to the iron takes place through the Nϵ2 atom. It is interesting that in ferrocytochrome c_2 from *Rhodospirillum rubrum* (reduced, diamagnetic form), the coordinated histidine (His-18) Nδ1H has a chemical shift of 170.9 ppm (Yu and Smith, 1990). The difference between this chemical shift and the pure type α shift is caused by heme ring current shift (~ -4.5 ppm) and hydrogen bond formation ($\sim$8 ppm). In the paramagnetic form of the protein (oxidized), the shift of the same nitrogen is 193.5 ppm, where in addition to the ring current shift and the hydrogen bonding contribution, a total paramagnetic shift of $\sim$22.6 ppm displaces the signal downfield. The detection of the Nδ1H in both systems demonstrates that the ^{15}N chemical shift is a potential marker for studies of heme proteins in which coordinated histidines participate in hydrogen bond networks crucial to the structure and the functional properties of the protein. Examples include peroxidases: cytochrome *c* peroxidase, horseradish peroxidase, and lignin peroxidase, where an invariant Asp residue hydrogen bonds to the δ1 nitrogen of the proximal histidine. This hydrogen bond imparts a larger anionic character to the axial ligands in peroxidases than in globins (Poulos and Kraut, 1980a) and is believed to be the major factor responsible for the low redox potentials in the peroxidases (Poulos and Kraut, 1980b; Finzel et al., 1984; Beck von Bodman et al., 1986; Banci et al., 1991; Poulos et al., 1993; Smulevich, 1993). Also visible in the ^1H–^{15}N HMQC spectrum is the backbone amide signal of His-93, at 127.8 ppm (^{15}N) and 13.88 ppm (^1H) (Fig. 4 *B*). This well-resolved cross-peak will be helpful in monitoring exchange and dynamics in the metcyano form of Mb.

A comparison of the nitrogen chemical shifts in the metcyano and metaquo forms, and with other protein shifts, indicates that the nitrogen chemical shift is negligibly affected by paramagnetic effects. This has been observed in the iron-sulfur clusters as well (Oh and Markley, 1990) and is expected for the shift experienced by a nucleus with a low magnetogyric ratio when the number of bonds to the paramagnetic center is large enough to prevent contact contribution. The only strongly deviating nitrogen shift is for the proximal histidine, where contact shift is present.

CONCLUSIONS

^1H–^{15}N HMQC data are valuable in investigations of the protonation and tautomeric state of the histidines of myoglobin in its paramagnetic and diamagnetic complexes. Mb contains several histidines residing in diverse environments and engaged in specific interactions, and therefore conclusions can be drawn about the limitations of the method. The similarity of type α and type β ^{15}N shifts among residues suggests that the hydrogen bond status of an imidazole ring cannot be established from the nitrogen chemical shifts alone. However, when the formation of a hydrogen bond can reasonably be ruled out on independent structural grounds, the tautomeric state composition can be estimated. It is also interesting that not all signals were detected in many of the experiments, in particular for those residues with large Nδ1H proportions in the tautomeric mixture. These residues require a combination of methods, for example, change in complexation state, change of protein source, or different NMR experiments. The improved characterization of the structure of Mb will provide the necessary basis for the interpretation of thermodynamic data.

We thank graciously Dr. Melanie J. Cocco for participation in the early phase of the work, Dr. Fong Shu for the gift of the sperm whale myoglobin gene, Michael Mayer for advice with the protein expression and preparation, and Dr. Christopher J. Falzone for help with the collection of NMR data and useful discussions. Dr. Yung-Hsiang Kao is gratefully acknowledged for his critical reading of the manuscript.

This work was supported by a grant from the National Institutes of Health (GM54217).

REFERENCES

Alei, M. J., L. O. Morgan, W. E. Wageman, and T. W. Whaley. 1980. pH dependence of ^{15}N NMR shifts and coupling constants in aqueous imidazole and 1-methylimidazole: comments on estimation of tautomeric equilibrium constants for aqueous histidine. *J. Am. Chem. Soc.* 102:2881–2887.

Annand, R. R., J. F. Kozlowski, V. J. Davisson, and J. M. Schwab. 1993. Mechanism-based inactivation of *Escherichia coli* β-hydroxydecanoyl thiol ester dehydrase: assignment of the imidazole ^{15}N NMR resonances and determination of the structure of the alkylated histidine. *J. Am. Chem. Soc.* 115:1088–1094.

Bachovchin, W. W. 1986. ^{15}N NMR spectroscopy of hydrogen-bonding interactions in the active site of serine proteases: evidence for a moving histidine mechanism. *Biochemistry.* 25:7751–7759.

Bachovchin, W. W., W. Y. L. Wong, S. Farr-Jones, A. B. Shenvi, and C. A. Kettner. 1988. Nitrogen-15 NMR spectroscopy of the catalytic-triad histidine of a serine protease in peptide boronic acid inhibitor complexes. *Biochemistry.* 27:7689–7697.

Banci, L., I. Bertini, P. Turano, M. Tien, and T. K. Kirk. 1991. Proton NMR investigation into the basis for the relatively high redox potential of lignin peroxidase. *Proc. Natl. Acad. Sci. U.S.A.* 88:6956–6960.

Barrick, D., F. M. Hughson, and R. L. Baldwin. 1994. Molecular mechanisms of acid denaturation: the role of histidine residues in the partial unfolding of apomyoglobin. *J. Mol. Biol.* 237:588–601.

Bashford, D., D. A. Case, C. Dalvit, L. Tennant, and P. E. Wright. 1993. Electrostatic calculations of side-chain pK_a values in myoglobin and comparison with NMR data for histidines. *Biochemistry.* 32:8045–8056.

Beck von Bodman, A., M. A. Schuler, D. R. Jollie, and S. G. Sligar. 1986. Synthesis, bacterial expression, and mutagenesis of the gene coding for mammalian cytochrome b_5. *Proc. Natl. Acad. Sci. USA.* 83:9443–9447.

Bhattacharya, S., and J. T. J. Lecomte. 1997. Temperature dependence of hisitidine ionization constants in myoglobin. *Biophys. J.* 73:3241–3258.

Blomberg, F., W. Maurer, and H. Rueterjans. 1977. Nuclear magnetic resonance investigation of ^{15}N-labeled histidine in aqueous solution. *J. Am. Chem. Soc.* 29:8149–8159.

Bodenhausen, G., and D. G. Ruben. 1980. Natural abundance nitrogen-15 NMR by enhanced heteronuclear spectroscopy. *Chem. Phys. Lett.* 69: 185–189.

Boschcov, P. W., W. S. Seodel, J. Muradian, M. Tominaga, A. C. M. Paiva, and L. Juliano. 1983. Ionization constants and thermodynamic parameters of histidine and derivatives. *Bioorg. Chem.* 12:34–44.

Botelho, L. H., S. H. Friend, J. B. Matthew, L. D. Lehman, G. I. H. Hanania, and F. R. N. Gurd. 1978. Proton nuclear magnetic resonance study of histidine ionizations in myoglobins of various species: comparison of observed and computed pK values. *Biochemistry.* 17:5197–5205.

Botelho, L. H., and F. R. N. Gurd. 1978. Proton nuclear magnetic resonance study of histidine ionizations in myoglobins of various species: specific assignment of individual resonances. *Biochemistry.* 17: 5188–5196.

Breslow, E. 1964. Changes in side chain reactivity accompanying the binding of heme to sperm whale apomyoglobin. *J. Biol. Chem.* 239: 486–496.

Brünger, A. T. 1992. X-PLOR Version 3.1: A System for X-Ray Crystallography and NMR. Yale University Press, New Haven, CT.

Brunori, M., G. Amiconi, E. Antonini, J. Wyman, R. Zito, and R. Fanelli. 1968. The transition between 'acid' and 'alkaline' ferric heme proteins. *Biochim. Biophys. Acta.* 154:315–322.

Cheng, X., and B. P. Schoenborn. 1991. Neutron diffraction study of carbonmonoxymyoglobin. *J. Mol. Biol.* 220:381–399.

Cocco, M. J., Y.-H. Kao, A. T. Phillips, and J. T. J. Lecomte. 1992. Structural comparison of apomyoglobin and metaquomyoglobin: pH titration of histidines by NMR spectroscopy. *Biochemistry.* 31: 6481–6491.

Cutnell, J. D., G. N. La Mar, and S. B. Kong. 1981. Proton nuclear magnetic resonance study of the relaxation behavior and kinetic lability of exchangeable protons in the heme pocket of cyanometmyoglobin. *J. Am. Chem. Soc.* 103:3567–3572.

Dalvit, C., and P. E. Wright. 1987. Assignment of resonances in the ^{1}H nuclear magnetic resonance spectrum of the carbon monoxide complex of sperm whale myoglobin by phase-sensitive two-dimensional techniques. *J. Mol. Biol.* 194:313–327.

Emerson, S. D., and G. N. La Mar. 1990. Solution structural characterization of cyanometmyoglobin: resonance assignment of heme cavity residues by two-dimensional NMR. *Biochemistry.* 29:1545–1555.

Evans, S. V., and G. D. Brayer. 1990. High-resolution study of the three-dimensional structure of horse heart metmyoglobin. *J. Mol. Biol.* 213:885–897.

Farr-Jones, S., W. Y. L. Wong, W. G. Gutheil, and W. W. Bachovchin. 1993. Direct observation of the tautomeric forms of histidine in ^{15}N NMR at low temperatures: comments on intramolecular hydrogen bonding and on tautomeric equilibrium constants. *J. Am. Chem. Soc.* 115: 6813–6819.

Finzel, B. C., T. L. Poulos, and J. Kraut. 1984. Crystal structure of yeast cytochrome c peroxidase refined at 1.7-Å resolution. *J. Biol. Chem.* 259:13027–13036.

Friend, S. H., and F. R. N. Gurd. 1979a. Electrostatic stabilization in myoglobin: pH dependence of summed electrostatic contributions. *Biochemistry.* 18:4612–4619.

Friend, S. H., and F. R. N. Gurd. 1979b. Electrostatic stabilization in myoglobin: interactive free energies between individual sites. *Biochemistry.* 18:4620–4630.

García-Moreno, B., L. X. Chen, K. L. March, R. S. Gurd, and F. R. N. Gurd. 1985. Electrostatic interactions in sperm whale myoglobin: site specificity, roles in structural elements, and external electrostatic potential distributions. *J. Biol. Chem.* 260:14070–14082.

Garrett, D. S., Y. J. Seok, D. I. Liao, A. Peterkofsky, A. M. Gronenborn, and G. M. Clore. 1997a. Solution structure of the 30 kDa N-terminal domain of enzyme I of the *Escherichia coli* phosphoenolpyruvate:sugar phosphotransferase system by multidimensional NMR. *Biochemistry.* 36:2517–2530.

Garrett, D. S., Y. J. Seok, A. Peterkofsky, G. M. Clore, and A. M. Gronenborn. 1997b. Identification by NMR of the binding surface for the histidine-containing phosphocarrier protein HPr on the N-terminal domain of enzyme I of the *Escherichia coli* phosphotransferase system. *Biochemistry.* 36:4393–4398.

Kao, Y.-H. 1994. A study of metaquomyoglobin in solution by NMR spectroscopy: structural properties and histidine ionization. Ph.D. Thesis, The Pennsylvania State University, University Park, PA. 242 pp.

Kao, Y.-H., and J. T. J. Lecomte. 1993. Determination of the zero-field splitting constant for proton NMR chemical shift analysis in metaquomyoglobin: the dipolar shift as a structural probe. *J. Am. Chem. Soc.* 115:9754–9762.

La Mar, G. N., H. Toi, and R. Krishnamoorthi. 1984. Proton NMR investigation of the rate and mechanism of heme rotation in sperm whale myoglobin: evidence for intramolecular reorientation about a heme twofold axis. *J. Am. Chem. Soc.* 106:6395–6401.

Lecomte, J. T. J., and M. J. Cocco. 1990. Structural features of the protoporphyrin-apomyoglobin complex: a proton NMR spectrosocpy study. *Biochemistry.* 29:11057–11067.

Lecomte, J. T. J., Y.-H. Kao, and M. J. Cocco. 1996. The native state of apomyoglobin described by proton NMR spectroscopy: the A-B-G-H interface of wild-type sperm whale apomyoglobin. *Proteins Struct. Funct. Genet.* 25:267–285.

Lecomte, J. T. J., and G. N. La Mar. 1987. 1H NMR probe for hydrogen bonding of distal residues to bound ligands in heme proteins: isotope effect on heme electronic structure of myoglobin. *J. Am. Chem. Soc.* 109:7219–7220.

Lee, B., and F. M. Richards. 1971. The interpretation of protein structures: estimation of static accessibility. *J. Mol. Biol.* 55:379–400.

Live, D. H., D. G. Davis, W. C. Agosta, and D. Cowburn. 1984. Long range hydrogen bond mediated effects in peptides: ^{15}N NMR study of gramicidin S in water and organic solvents. *J. Am. Chem. Soc.* 106: 1939–1941.

Loewenthal, R., J. Sancho, and A. R. Fersht. 1992. Histidine-aromatic interactions in barnase: elevation of histidine pK_a and contribution to protein stability. *J. Mol. Biol.* 224:759–770.

Martin, M. L., G. J. Martin, and J.-J. Delpuech. 1980. Practical NMR Spectroscopy. Heyden, Philadelphia.

McGrath, T. M., and G. N. La Mar. 1978. Proton NMR study of the thermodynamics and kinetics of the acid in equilibrium base transitions in reconstituted metmyoglobins. *Biochim. Biophys. Acta.* 534:99–111.

Morikis, D., P. M. Champion, B. A. Springer, and S. G. Sligar. 1989. Resonance raman investigations of site-directed mutants of myoglobin: effects of distal histidine replacement. *Biochemistry.* 28:4791–800.

Müller, L. 1979. Sensitivity enhanced detection of weak nuclei using heteronuclear multiple quantum coherence. *J. Am. Chem. Soc.* 101: 4481–4484.

Oh, B.-H., and J. L. Markley. 1990. Multinuclear magnetic resonance studies of the 2Fe-2S* ferredoxin from *Anabaena* species strain PCC 7120. III. Detection and characterization of hyperfine-shifted nitrogen-15 and hydrogen-1 resonances of the oxidized form. *Biochemistry.* 29:4012–4017.

Pelton, J. G., D. A. Torchia, N. D. Meadow, and S. Roseman. 1993. Tautomeric states of the active-site histidines of phosphorylated and unphosphorylated IIIGlc, a signal-transducing protein from *Escherichia coli*, using two-dimensional heteronuclear NMR techniques. *Protein Sci.* 2:543–558.

Phillips, S. E. V. 1980. The structure and refinement of oxymyoglobin at 1.6 angstrom resolution. *J. Mol. Biol.* 142:531–554.

Piotto, M., V. Saudek, and V. Sklenar. 1992. Gradient-tailored excitation for single-quantum NMR spectroscopy of aqueous solutions. *J. Biomol. NMR.* 2:661–665.

Plesniak, L. A., G. P. Connelly, W. W. Wakarchuck, and L. P. McIntosh. 1996. Characterization of a buried neutral histidine residue in *Bacillus circulans* xylanase: NMR assignments, pH titration, and hydrogen exchange. *Protein Sci.* 5:2319–2328.

Poulos, T. L., S. L. Edwards, H. Wariishi, and M. H. Gold. 1993. Crystallographic refinement of lignin peroxidase at 2 Å. *J. Biol. Chem.* 268:4429–4440.

Poulos, T. L., and J. Kraut. 1980a. The stereochemistry of peroxidase catalysis. *J. Biol. Chem.* 255:8199–8205.

Poulos, T. L., and J. Kraut. 1980b. A hypothetical model of the cytochrome *c* peroxidase/cytochrome *c* electron transfer complex. *J. Biol. Chem.* 255:10322–10330.

Reynolds, W. F., I. R. Peat, M. H. Freedman, and J. R. Lyerla. 1973. Determination of the tautomeric form of the imidazole ring of L-histidine in basic solution by carbon-13 magnetic resonance spectroscopy. *J. Am. Chem. Soc.* 95:328–331.

Roberts, J. D., C. Yu, C. Flanagan, and T. R. Birdseye. 1982. A nitrogen-15 NMR study of acid-base and tautomeric equilibria of 4-substituted imidazoles and its relevance to the catalytic mechanism of α-lytic protease. *J. Am. Chem. Soc.* 104:3945–3949.

Sambrook, J., E. F. Fritsch, and T. Maniatis. 1989. Molecular Cloning: A Laboratory Manual. Cold Spring Harbor Laboratory Press, Cold Spring Harbor, NY.

Shire, S. J., G. I. H. Hanania, and F. R. N. Gurd. 1974. Electrostatic effects in myoglobin: hydrogen ion equilibria in sperm whale ferrimyoglobin. *Biochemistry.* 13:2967–2979.

Shuster, I. I., and J. D. Roberts. 1979. Nitrogen-15 NMR spectroscopy: effects of hydrogen bonding and protonation on nitrogen chemical shifts in imidazole. *J. Org. Chem.* 44:3864–3867.

Smith, S. O., S. Farr-Jones, R. G. Griffin, and W. W. Bachovchin. 1989. Crystal versus solution structures of enzymes: NMR spectroscopy of a crystalline serine protease. *Science.* 244:961–963.

Smulevich, G. 1993. Biomolecular Spectroscopy, Part A. John Wiley and Sons, London.

Sudmeier, J. L., E. L. Ash, U. L. Guenther, L. X., P. A. Bullock, and W. W. Bachovchin. 1996. HCN, A triple-resonance NMR technique for selective observation of histidine and tryptophan side chains in $^{13}C/^{15}N$-labeled proteins. *J. Magn. Reson. B.* 113:236–247.

Takano, T. 1977a. Structure of myoglobin refined at 2.0 Å resolution. I. Crystallographic refinement of sperm whale metmyoglobin. *J. Mol. Biol.* 110:537–568.

Takano, T. 1977b. Structure of myoglobin refined at 2.0 Å resolution. II. Structure of deoxymyoglobin from sperm whale. *J. Mol. Biol.* 110: 569–584.

Takano, T. 1984. Refinement of myoglobin and cytochrome *c*. *In* Methods and Applications in Crystallographic Computing. Oxford University Press, Oxford, U.K. 262–272.

Tanokura, M. 1983. ^{1}H-NMR study on the tautomerism of the imidazole ring of histidine residues. I. Microscopic pK values and molar ratios of tautomers in histidine-containing peptides. *Biochim. Biophys. Acta.* 742: 576–585.

Teale, F. W. J. 1959. Cleavage of heme-protein link by acid methylethylketone. *Biochim. Biophys. Acta.* 35:543.

Tolman, J. R., J. M. Flanagan, M. A. Kennedy, and J. H. Prestegard. 1995. Nuclear magnetic dipole interactions in field-oriented proteins: information for structure determination in solution. *Proc. Natl. Acad. Sci. USA.* 92:9279–9283.

van Dijk, A. A., L. C. M. de Lange, W. W. Bachovchin, and G. T. Robillard. 1990. Effect of phosphorylation on hydrogen-bonding interactions of the active site histidine of HPr determined by ^{15}N NMR spectroscopy. *Biochemistry.* 29:8164–8171.

van Dijk, A. A., R. M. Scheek, K. Dijkstra, G. K. Wolters, and G. T. Robillard. 1992. Characterization of the protonation and hydrogen bonding state of the histidines in IIAmtl, a domain of the phosphoenolpyruvate-dependent mannitol-specific transport protein. *Biochemistry.* 31: 9063–9072.

Vuister, G. W., and A. Bax. 1992. Resolution enhancement and spectral editing of uniformly ^{13}C-enriched proteins by homonuclear broadband ^{13}C decoupling. *J. Magn. Reson.* 98:428–435.

Wasylishen, R. E., and G. Tomlinson. 1975. pH-dependence of ^{13}C chemical shifts and $^{13}C,H$ coupling constants in imidazole and L-histidine. *Biochem. J.* 147:605–607.

Wasylishen, R. E., and G. Tomlinson. 1977. Application of long-range $^{13}C,H$ nuclear spin-spin coupling constants in the study of imidazole tautomerism in L-histidine, histamine, and related compounds. *Can. J. Biochem.* 147:579–582.

Wilbur, D. J., and A. Allerhand. 1977. Titration behavior and tautomeric states of individual histidine residues of myoglobin. *J. Biol. Chem.* 252:4968–4975.

Wishart, D. S., C. G. Bigam, J. Yao, F. Abildgaard, H. J. Dyson, E. Oldfield, J. L. Markley, and B. D. Sykes. 1995. ^{1}H, ^{13}C and ^{15}N chemical shift referencing in biomolecular NMR. *J. Biomol. NMR.* 6:135–140.

Witanowski, M., L. Stefaniak, H. Januszewski, Z. Grabowski, and G. A. Webb. 1972. Nitrogen-14 nuclear magnetic resonance of azoles and their benzo derivatives. *Tetrahedron.* 28:637–653.

Wüthrich, K. 1986. NMR of Proteins and Nucleic Acids. Wiley, New York.

Xia, B., H. Cheng, L. Skjeldal, V. M. Coghlan, L. E. Vickery, and J. L. Markley. 1995. Multinuclear magnetic resonance and mutagenesis studies of the histidine residues of human mitochondrial ferredoxin. *Biochemistry.* 34:180–187.

Yamamoto, Y. 1996. ^{1}H NMR probes for the inter-segmental hydrogen bonds in myoglobin. *J. Biochem.* 120:126–132.

Yang, A.-S., and B. Honig. 1994. Structural origins of pH and ionic strength effects on protein stability: acid denaturation of sperm whale apomyoglobin. *J. Mol. Biol.* 237:602–614.

Yang, F., and G. N. J. Phillips. 1996. Crystal structures of CO-, deoxy- and met-myoglobins at various pH values. *J. Mol. Biol.* 256:762–774.

Yu, L. P., and G. M. Smith. 1990. Characterization of pH-dependent conformational heterogeneity in *Rhodospirillum rubrum* cytochrome c_2 using ^{15}N and ^{1}H NMR. *Biochemistry.* 29:2920–2925.